

Phase transitions and molecular motions in $[\text{Ni}(\text{ND}_3)_6](\text{ClO}_4)_2$ [☆]

Anna Migdał-Mikuli,^{a,*} Edward Mikuli,^a Natalia Górska,^a Aneta Kowalska,^b
and Jacek Ulański^b

^a Department of Chemical Physics, Faculty of Chemistry, Jagiellonian University, Ulica Ingardena 3, Kraków 30-060, Poland

^b Department of Molecular Physics, Faculty of Chemistry, Technical University of Łódź, Żeromskiego 116, Łódź 90-924, Poland

Received 23 February 2004; received in revised form 6 April 2004; accepted 13 April 2004

Abstract

$[\text{Ni}(\text{ND}_3)_6](\text{ClO}_4)_2$ has three solid phases between 100 and 300 K. The phase transitions temperatures at heating ($T_{\text{C}1}^{\text{h}} = 164.1$ K and $T_{\text{C}2}^{\text{h}} = 145.1$ K) are shifted, as compared to the non-deuterated compound, towards the lower temperature of ca. 8 and 5 K, respectively. The ClO_4^- anions perform fast, picosecond, isotropic reorientation with the activation energy of 6.6 kJ mol^{-1} , which abruptly slow down at $T_{\text{C}1}^{\text{c}}$ phase transition, during sample cooling. The ND_3 ligands perform fast uniaxial reorientation around the Ni–N bond in all three detected phases, with the effective activation energy of 2.9 kJ mol^{-1} . The reorientational motion of ND_3 is only slightly distorted at the $T_{\text{C}1}$ phase transition due to the dynamical orientational order–disorder process of anions. The low value of the activation energy for the ND_3 reorientation suggests that this reorientation undergoes the translation–rotation coupling, which makes the barrier to the rotation of the ammonia ligands not constant but fluctuating. The phase polymorphism and the dynamics of the molecular reorientations of the title compound are similar but not quite identical with these of the $[\text{Ni}(\text{NH}_3)_6](\text{ClO}_4)_2$.

© 2004 Elsevier Inc. All rights reserved.

Keywords: Hexaaminenickel(II) chlorate(VII) deuterated; Phase transitions; Molecular reorientations; DSC; Raman scattering spectroscopy; Fourier transform far- and middle-infrared spectroscopy

1. Introduction

So far the title compound has only been the object of infrared and Raman investigations [1]. However, the phase transitions and molecular motions were investigated widely for the non-deuterated compound by Janik's [2–9] and Stankowski's [10–13] scientific teams. Two phase transitions were detected for $[\text{Ni}(\text{NH}_3)_6](\text{ClO}_4)_2$ by adiabatic calorimetry measurements: at $T_{\text{C}1}^{\text{h}} = 173.05$ K and at $T_{\text{C}2}^{\text{h}} = 143.0$ K, which were connected with big and small anomalies of the heat capacity $C_5(T)$, respectively [2]. Reorientational motions of the NH_3 ligands were measured by quasi-elastic neutron scattering (QENS) [3–6], by infrared [7] and by Raman spectroscopy [8]. At room temperature, the

reorientational correlation time for 120° jumps of NH_3 molecules around the threefold axis is of an order of 10^{-12} s and gets longer, with the activation energy $E_a \approx 4 \text{ kJ mol}^{-1}$, when the temperature goes down. This reorientation does not change much at both phase transitions. Reorientational motions of ClO_4^- anions were measured by Raman spectroscopy [8]. Reorientational correlation time for ClO_4^- anions at room temperature is ca. 3×10^{-12} s and gets longer as the temperature is going down with $E_a \approx 6 \text{ kJ mol}^{-1}$. It was observed that, contrary to the NH_3 ligands, the reorientation of ClO_4^- anions during the cooling suddenly slows down at $T_{\text{C}1}$ phase transition [8]. The high-temperature phase transition was also observed by EPR [10,11] and dilatometric [12] measurements. At $T_{\text{C}1}$ the $[\text{Ni}(\text{NH}_3)_6](\text{ClO}_4)_2$ also changes its crystal structure from regular-cubic ($Fm\bar{3}m$, No. 225) to monoclinic ($P2_1/c$, No. 14) [9,13].

The aim of the present study was to determine the phase polymorphism of the title compound, to find its

[☆]The paper is dedicated to the memory of Professor Janina Maria Janik (1925–1993).

*Corresponding author.

E-mail address: mikuli@chemia.uj.edu.pl (A. Migdał-Mikuli).

connection with reorientational motions of the ND_3 ligands and ClO_4^- anions, and finally to compare the obtained results with those for the non-deuterated compound. The investigations were performed with differential scanning calorimetry (DSC) and Fourier transform far- and mid-infrared (FT-FIR and FT-MIR) spectroscopy and Raman scattering (FT-RS and RS) spectroscopy.

2. Experimental

The examined compound was obtained by adding a heavy ammonia solution, drop by drop, to a concentrated solution of $[\text{Ni}(\text{D}_2\text{O})_6](\text{ClO}_4)_2$ in heavy water, which was cooled with a mixture of NaCl and ice. $[\text{Ni}(\text{D}_2\text{O})_6](\text{ClO}_4)_2$ was earlier synthesized by Rachwalska [14]. The precipitated small crystals, violet in color, were filtrated and dried over BaO. Before the measurements, the composition of the compound was determined on the basis of nickel and ammonia content, with titration by means of EDTA and HCl, respectively. The average contents of nickel and ammonia were found to be equal to the theoretical values within the error limit of ca. 1% and 3%, respectively. Non-deuterated compound was synthesized earlier by Pytasz [2].

The DSC measurements at 95–300 K were performed with a Perkin-Elmer PYRIS 1 DSC apparatus. The experimental details were the same as published in Ref. [15].

The infrared absorption measurements (FT-FIR and FT-MIR) were performed with a Digilab FTS-14 and Bruker EQUINOX 55 Fourier transform infrared spectrometers. The measurements were made at a resolution of 2 cm^{-1} . The FT-FIR spectra for powder samples suspended in Apiezon grease were recorded. Polyethylene and silicon windows were used. The FT-MIR spectra were recorded for the powdered sample suspended in KBr pellet. A He-cryostats with controlled heating and cooling rates and temperature stabilization within 0.2 K were used to obtain spectra for low temperatures. The temperature of the “cold finger” was measured with $\pm 1\text{ K}$ accuracy, but the temperature of the sample could be several Kelvin higher.

Fourier transform Raman scattering measurements (FT-RS) were performed at room temperature with a Bio-Rad spectrometer, resolution 4 cm^{-1} . The incident radiation ($\lambda = 1064\text{ nm}$) was from the Neodymium laser YAG Spectra-Physics. The Raman scattering measurements in the function of temperature were performed with Micro-Raman Spectrometer (Jobin-Yvon 64000). The incident radiation ($\lambda = 514.5\text{ nm}$) was from the Argon laser (LEXEL). The samples were mounted by grease on a cold stage in a homemade helium cryostat, and cooled down.

The X-ray powder diffraction (XRPD) pattern at RT was obtained with a Seifert XRD-7 diffractometer using Ni-filtrated $\text{CuK}\alpha$ radiation.

3. Results and discussion

3.1. Identification of the compound

The XRPD pattern of $[\text{Ni}(\text{ND}_3)_6](\text{ClO}_4)_2$ at room temperature can be indexed in a regular (cubic) system, space group No. 225 = $Fm\bar{3}m = O_h^5$, with four formula units in a unit cell of edge $a = 11.4590 \pm 0.0007\text{ \AA}$. At room temperature $[\text{Ni}(\text{NH}_3)_6](\text{ClO}_4)_2$ has the same space group, but the lattice parameter a equal to: 11.41 \AA [9], 11.42 \AA [13] and 11.44 \AA [16].

Fig. 1 shows a comparison of Raman (FT-RS) and infrared (FT-FIR and FT-MIR) spectra of $[\text{Ni}(\text{ND}_3)_6](\text{ClO}_4)_2$ obtained at room temperature. There are 69 normal modes for the octahedral complex cation of O_h symmetry: $3A_{1g} + A_{1u} + 3E_g + E_u + 4F_{1g} + 7F_{1u} + 4F_{2g} + 4F_{2u}$, but $3F_{1g}$ and $4F_{2u}$ are Raman and infrared inactive, respectively. Six of them ($A_{1u} + E_u + F_{1g}$) are connected with the torsions of the ND_3 ligands. The ClO_4^- anion has 9 normal modes: A_1 , E and $2F_2$. Two first are infrared inactive but all of them are active in the Raman spectrum. The cation was considered to have octahedral symmetry with freely rotating ND_3 ligands, while the anion had tetrahedral

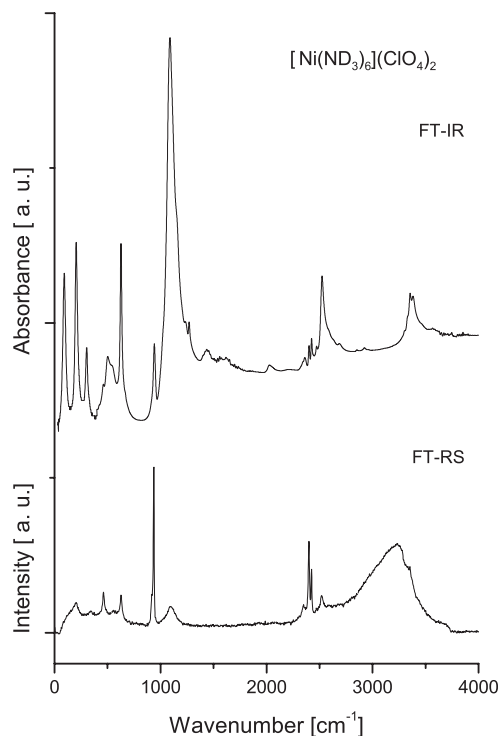


Fig. 1. Comparison of the infrared (FT-FIR and FT-MIR) and Raman (FT-RS) spectra for $[\text{Ni}(\text{ND}_3)_6](\text{ClO}_4)_2$ at room temperature.

Table 1

List of band positions of the Raman (FT-RS) and infrared (FT-MIR and FT-FIR) spectra of $[\text{Ni}(\text{ND}_3)_6](\text{ClO}_4)_2$ at room temperature and the comparison with the literature data

Frequencies (cm^{-1})		Assignments	
RS	IR		
This work	[1]	This work	
		3381 m	$\nu_{\text{as}}(\text{NH})F_{1u}$
		3355 m	$\nu_{\text{s}}(\text{NH})F_{1u}$
3350 sh			$\nu_{\text{as}}(\text{NH})F_{1g}$
3200 br			$\nu_{\text{s}}(\text{NH})A_{1g}$
		2524 st	$\nu_{\text{as}}(\text{ND})F_{1u}$
2517 m	2523		$\nu_{\text{as}}(\text{ND})F_{2g}$
	2475	2470 sh	
2424 st	2430		$\nu_{\text{s}}(\text{ND})E_g$
		2425 m	$\nu_{\text{s}}(\text{ND})F_{1u}$
2399 vst	2405		$\nu_{\text{s}}(\text{ND})A_{1g}$
		2401 m	$2\delta_{\text{as}}(\text{DND})F_{1u}$
2349 w	2350	2360 w	$2\delta_{\text{as}}(\text{DND})F_{2g}$
		1620 w, br	$\delta_{\text{as}}(\text{HNH})F_{1u}$
		1436 w, br	$\delta_{\text{as}}(\text{DNH})F_{1u}$
		1267 m	$\delta_{\text{as}}(\text{DND})F_{1u}$
		1236 sh	
1100 m, br ^a	1100 ^a		$\delta_{\text{as}}(\text{DND})F_{2g}$
1096 m, br	—	1089 vst	$\nu_{\text{as}}(\text{ClO})F_2$
		941 st ^b	$\delta_{\text{s}}(\text{DND})F_{1u}$
			$\delta_{\text{s}}(\text{DND})E_g$
			$\delta_{\text{s}}(\text{DND})A_{1g}$
940 w ^b	—		$\nu_{\text{s}}(\text{ClO})A_1$
937 vst	940	941 st	$2\delta_{\text{d}}(\text{OCIO})E + A_1$
918 sh	920		$\delta_{\text{d}}(\text{OCIO})F_2$
627 st	630	627 vst	$\nu_{\text{s}}(\text{NiN})E_g$
555 w	—	555 w	$\rho_{\text{r}}(\text{ND}_3)F_{2g}$
?	—		$\rho_{\text{r}}(\text{ND}_3)F_{1u}$
		502 m	$\delta_{\text{d}}(\text{OCIO})E$
461 st	465	461 w	$\nu_{\text{s}}(\text{NiN})A_{1g}$
339 w	340		$\nu_{\text{as}}(\text{NiN})F_{1u}$
		302 m	$\delta_{\text{as}}(\text{NNiN})F_{2g}$
203 m	217		$\delta_{\text{as}}(\text{NNiN})F_{1u}$
		204 st	$\nu_{\text{L}}(\text{lattice})F_{2g}$
152 sh	—		
		92 st	$\nu_{\text{L}}(\text{lattice})F_{1u}$

vw—very weak, w—weak, sh—shoulder, m—medium, st—strong, vst—very strong, br—broad. There exist also some bands which belong to the non-deuterated compound because of the only 95% deuteration.

^a Perhaps mixed with $\nu_{\text{as}}(\text{ClO})F_2$.

^b Perhaps mixed with $\nu_{\text{s}}(\text{ClO})A_1$.

symmetry. Table 1 presents the list of the bands positions observed in the FT-RS and FT-FIR plus FT-MIR spectra of $[\text{Ni}(\text{ND}_3)_6](\text{ClO}_4)_2$ and their relative intensities and assignments fixed by comparing with the literature data [1,17,18]. An isotopic shift of ND_3 internal vibrations frequencies was observed such as it was expected. These assignments, besides the XRPD data, proved that both the composition and the structure of the investigated compound were the same as expected.

3.2. Phase transitions measurements

The DSC measurements were made both on heating and cooling the fresh synthesized $[\text{Ni}(\text{ND}_3)_6](\text{ClO}_4)_2$ sample of mass equal to 14.26 mg at constant rates of 10, 20, 30 and 40 K min^{-1} . Fig. 2 presents the temperature dependences of the heat flow (DSC curves) obtained for the title compound on heating (upper curve) and on cooling (down curve) at the rate of 20 K min^{-1} . Two distinct anomalies were registered on each of these two DSC curves at: $T_{\text{C1}}^{\text{c}} = 160.2 \text{ K}$ and $T_{\text{C2}}^{\text{c}} = 142.1 \text{ K}$ (on cooling) and at: $T_{\text{C1}}^{\text{h}} = 164.7 \text{ K}$ and $T_{\text{C2}}^{\text{h}} = 145.1 \text{ K}$ (on heating). The phase transition temperatures: T_{C1}^{h} , T_{C2}^{h} and T_{C1}^{c} , T_{C2}^{c} were calculated by extrapolating the corresponding T_{C}^{h} and T_{C}^{c} values versus the scanning rate dependences, registered at four scanning rates of heating and cooling the sample: 10, 20, 30 and 40 K min^{-1} , to the scanning rate value equal to zero K min^{-1} . The presence of ca. 4 and 3 K hysteresis of the T_{C1} and T_{C2} phase transition temperature, respectively, suggests that the detected phase transitions are of the

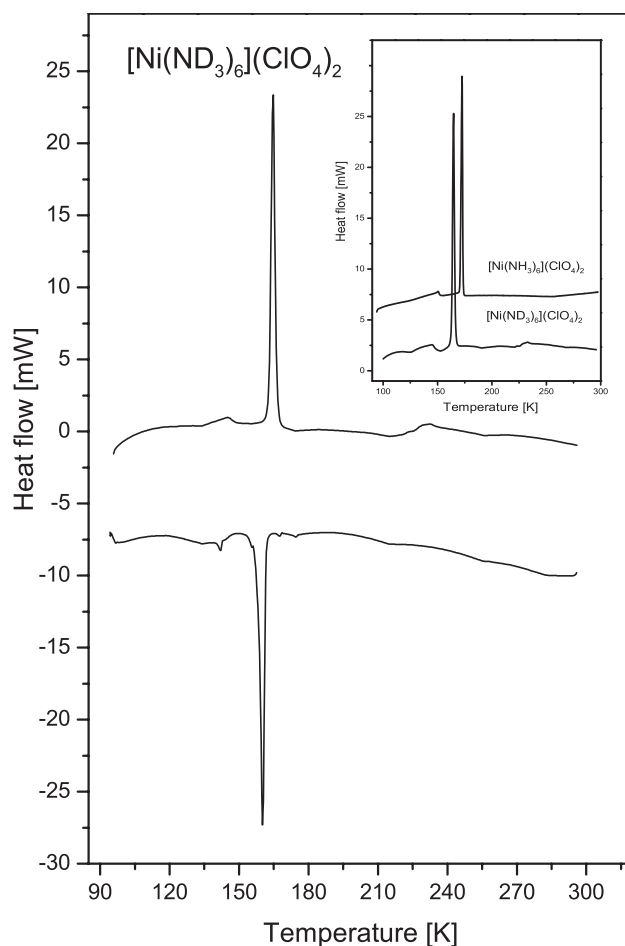


Fig. 2. DSC curves for $[\text{Ni}(\text{ND}_3)_6](\text{ClO}_4)_2$ obtained at cooling (lower curve) and heating (upper curve) at a constant scanning rate of 20 K min^{-1} . Inset: comparison of the DSC curves for $[\text{Ni}(\text{ND}_3)_6](\text{ClO}_4)_2$ and $[\text{Ni}(\text{NH}_3)_6](\text{ClO}_4)_2$.

Table 2

Thermodynamic parameters of the phase transitions of $[\text{Ni}(\text{ND}_3)_6](\text{ClO}_4)_2$ and $[\text{Ni}(\text{NH}_3)_6](\text{ClO}_4)_2$

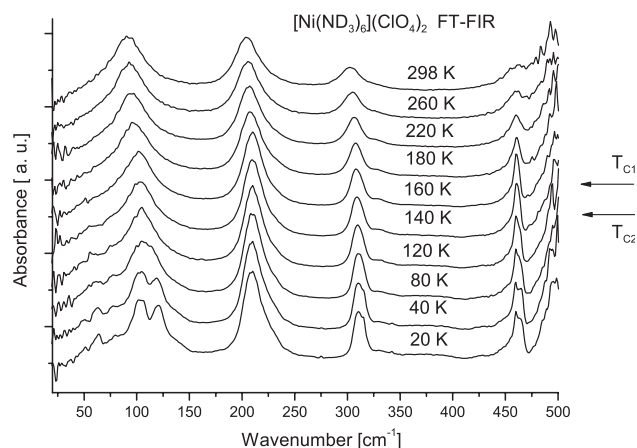
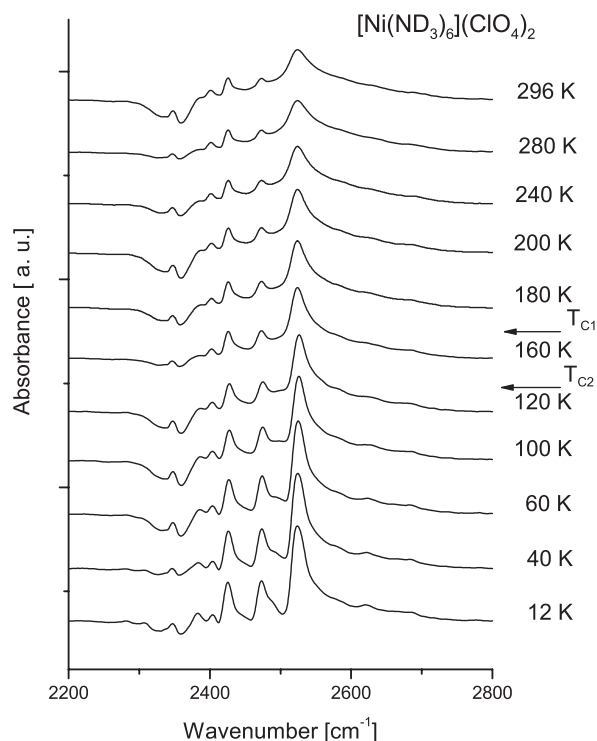
	$[\text{Ni}(\text{ND}_3)_6](\text{ClO}_4)_2$		$[\text{Ni}(\text{NH}_3)_6](\text{ClO}_4)_2$		
	Heating	Cooling	Heating	Cooling	Heating ^a
T_{C1} (K)	164.1 ± 0.1	161.1 ± 0.1	172.5 ± 0.1	168.8 ± 0.1	173.05 ± 0.05
T_{C2} (K)	145.1 ± 0.1	142.1 ± 0.1	150.5 ± 0.1	149.6 ± 0.1	143.00 ± 0.15
ΔH_1 (kJ mol ⁻¹)	5.1 ± 0.1	5.1 ± 0.1	5.4 ± 0.1	5.6 ± 0.1	5.65 ± 0.20
ΔH_2 (kJ mol ⁻¹)	0.4 ± 0.1	0.4 ± 0.1	0.7 ± 0.2	0.6 ± 0.2	0.54 ± 0.03
ΔS_1 (J mol ⁻¹ K ⁻¹)	31.2 ± 0.3	31.8 ± 0.3	31.5 ± 0.8	33.1 ± 0.8	32.64 ± 1.17
ΔS_2 (J mol ⁻¹ K ⁻¹)	2.8 ± 0.5	2.8 ± 0.5	4.4 ± 1.2	4.3 ± 1.2	3.76 ± 0.25

^aAdiabatic calorimetry results [2].

first-order type. The thermodynamic parameters of the detected phase transitions are presented in Table 2. Thus, the title compound has three solid phases: high temperature (phase I), intermediate (phase II) and low-temperature phase (phase III). Additionally, the DSC curves were registered at heating and cooling of $[\text{Ni}(\text{NH}_3)_6](\text{ClO}_4)_2$ sample of mass equal to 13.97 mg with a scanning rate of 20 K min⁻¹. The inset in Fig. 2 presents a comparison of the DSC curves for deuterated and non-deuterated hexaaminenickel(II) chlorate(VII) recorded at heating at the same scanning rate. We can observe a shift of both anomalies to lower temperature after deuteration. Table 2 also contains the thermodynamic parameters for the non-deuterated compound.

3.3. Structure and reorientational dynamics changes

The FT-FIR spectra were recorded during the heating and cooling of the sample. Fig. 3 shows exemplarily the spectra obtained at several chosen temperatures only during the heating. Some evident changes of the spectra at the temperature region of the both phase transitions can be noticed. Namely, apart from of the narrowing, the splitting of some bands can be seen below the phase transitions. The FT-MIR spectra were recorded only during sample cooling. Fig. 4 presents the bands connected with the ND stretching modes from FT-MIR spectra obtained at several chosen temperatures. Appearing of a new band at the vicinity of 2490 cm⁻¹ and narrowing of some bands can be noticed in the spectra in the region of the both phase transitions. Thus, according to the infrared spectroscopy point of view a change of the crystal structure takes place at the phase transitions. The Raman spectra versus temperature (from 300 to 80 K) were also recorded. Fig. 5 presents several chosen Raman spectra vs. temperature in the frequency region of 200–800 cm⁻¹. The splitting, besides the narrowing of two broad bands connected with $\delta_{\text{d}}(\text{OCIO})E$ and $\delta_{\text{d}}(\text{OCIO})F_2$ modes at ca. 460 and 630 cm⁻¹, respectively, with lowering of temperature can be distinctly observed. Fig. 6 presents temperature dependencies of these two peaks positions. It can be clearly seen that the $\delta_{\text{d}}(\text{OCIO})E$ band splits on two

Fig. 3. Temperature dependence of the FT-FIR spectra of $[\text{Ni}(\text{ND}_3)_6](\text{ClO}_4)_2$.Fig. 4. Temperature dependence of the N-D stretching bands region of the FT-MIR spectra of $[\text{Ni}(\text{ND}_3)_6](\text{ClO}_4)_2$.

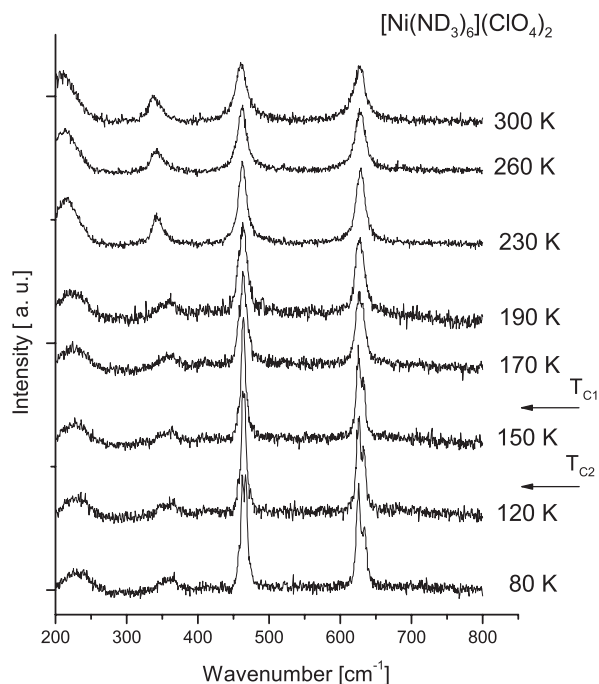


Fig. 5. Temperature dependence of the RS spectra of $[\text{Ni}(\text{ND}_3)_6](\text{ClO}_4)_2$ at frequency region of 200–800 cm^{-1} .

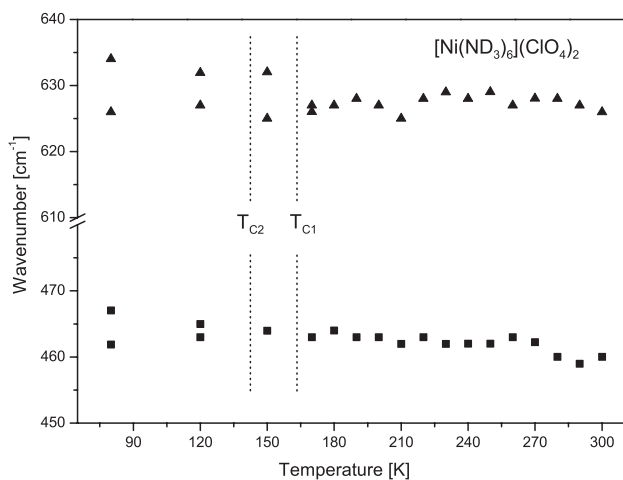


Fig. 6. Temperature dependences of bands positions for $\delta_d(\text{OCIO})E$ and $\delta_d(\text{OCIO})F_2$ modes in 450–470 cm^{-1} and 610–630 cm^{-1} wavenumber range, respectively.

components below the phase transition at T_{C2} and the $\delta_d(\text{OCIO})F_2$ band splits just below the phase transition at T_{C1} . The splitting of these bands suggests that the crystal symmetry is reduced.

Moreover, the narrowing of the bands connected with $\delta_d(\text{OCIO})E$ and $\delta_d(\text{OCIO})F_2$ modes implies “freezing” of the fast reorientational motions of the ClO_4^- anions. We would like to verify whether the observed phase transitions are connected or not with a change of the reorientational dynamics of the ND_3 ligands and/or the ClO_4^- anions. The question is also whether the

reorientation occurs in a similar way as in the case of $[\text{Ni}(\text{NH}_3)_6](\text{ClO}_4)_2$ and other compounds of the type: $[\text{M}(\text{NH}_3)_6](\text{XY}_4)_2$ [6], where the molecular groups demonstrate the so called dynamical orientational disorder. Studies of the temperature dependence of the full width at half maximum (FWHM) for three modes: $\nu_{\text{as}}(\text{ND})F_{1u}$ (at ca. 2524 cm^{-1}), $\delta_d(\text{OCIO})E$ (at ca. 460 cm^{-1}) and $\delta_d(\text{OCIO})F_2$ (at ca. 630 cm^{-1}) were made in order to obtain answers to the above questions.

We follow the analysis of FWHM described by Carabatos-Nédelec and Becker [19], which is based on the theory used for the damping associated with an order-disorder mechanism. We assumed that the reorientational correlation time τ_R is the mean time between the instantaneous jumps from one potential well to the other, and it is defined as $\tau_R = \tau_0 \exp(E_a/k_B T)$, where τ_0 is the relaxation time at infinite temperature T , E_a is the height of the potential barrier for ligands or anions reorientation and k_B is the Boltzmann constant. For a chosen phonon mode of the ω frequency, if $\omega^2 \tau_R^2 \gg 1$, the temperature dependence of the FWHM of the infrared and Raman bands connected with this mode can be described by [20–22]

$$\text{FWHM}(T) = (a + bT) + c \exp\left(-\frac{E_a}{k_B T}\right), \quad (1)$$

where a , b , c and E_a are parameters to fit. The linear part of Eq. (1) corresponds to the bandwidth connected with the vibrational relaxation and the exponential term corresponds to the bandwidth connected with the reorientational relaxation.

The FWHM of the bands connected with $\delta_d(\text{OCIO})E$, $\delta_d(\text{OCIO})F_2$ and $\nu_{\text{as}}(\text{ND})F_{1u}$ modes at several different temperatures of the RS and FT-MIR measurements were calculated by fitting the Lorentz function to the band using the GRAMS 32 v5.2 procedure. Figs. 7 and 8 present the temperature dependences of the FWHM

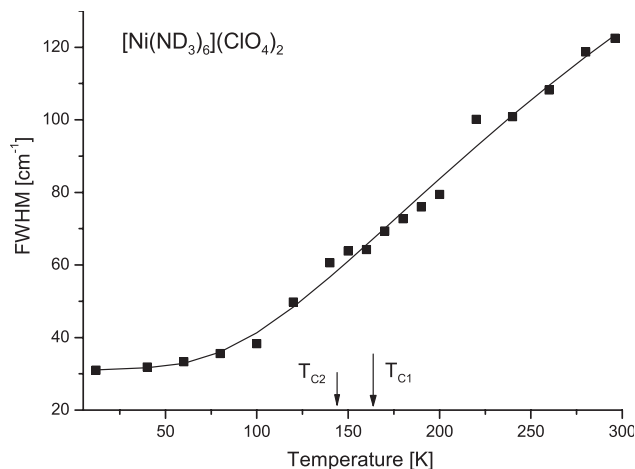


Fig. 7. Temperature dependence of the FWHM of the band at 2524 cm^{-1} connected with $\nu_{\text{as}}(\text{ND})F_{1u}$ mode.

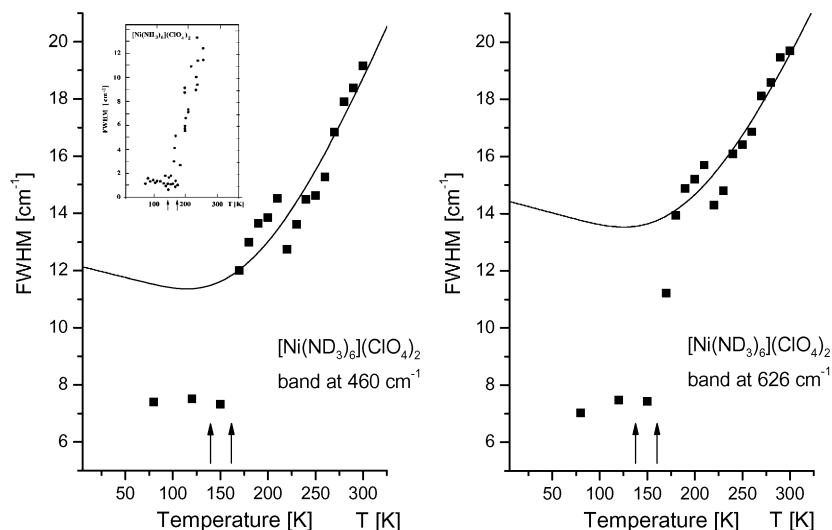


Fig. 8. Temperature dependences of the FWHM of the bands: (a) at 460 cm^{-1} connected with $\delta_d(\text{OCIO})E$ mode, (b) at 630 cm^{-1} connected with $\delta_d(\text{OCIO})F_2$ mode for $[\text{Ni}(\text{ND}_3)_6](\text{ClO}_4)_2$. Insertion presents temperature dependence of the FWHM of the band at 460 cm^{-1} connected with $\delta_d(\text{OCIO})E$ mode for $[\text{Ni}(\text{NH}_3)_6](\text{ClO}_4)_2$.

Table 3

Fitted parameters a , b , c and E_a for the temperature dependences of the FWHM of the bands connected with $\nu_{\text{as}}(\text{ND})F_{1u}$, $\delta_d(\text{OCIO})E$ and $\delta_d(\text{OCIO})F_2$ modes

Modes Phases	$\nu_{\text{as}}(\text{ND})F_{1u}$ I, II and III	$\delta_d(\text{OCIO})E$ I	$\delta_d(\text{OCIO})F_2$ I
a (cm^{-1})	30.8	12.2	14.5
b ($\text{cm}^{-1}\text{ K}^{-1}$)	21.1×10^{-3}	-8.3×10^{-3}	-8.9×10^{-3}
c ($\text{cm}^{-1}\text{ K}^{-1}$)	283.8	119.2	120.4
E_a (kJ mol^{-1})	2.9	6.4	6.8

for the three chosen bands. The solid lines in Figs. 7 and 8 are fitted by Eq. (1). The fitted parameters are listed in Table 3.

It can be seen in Fig. 7 that the FWHM value exponentially decreases while the temperature is being reduced down to 40 K and then becomes nearly constant. It means that the fast ND_3 reorientation “survives” the phase transitions. The estimated value of the activation energy for the reorientation of the ND_3 ligands is $E_a = 2.9\text{ kJ mol}^{-1}$ (0.7 kcal mol^{-1}) in phases I–III. The obtained values are very close to those for $[\text{Ni}(\text{NH}_3)_6](\text{ClO}_4)_2$ ($E_a = 4\text{ kJ mol}^{-1}$ [6]) and also to those for other hexaaminemetal(II) and hexaaminemetal(III) chlorates(VII), for example $E_a = 2.3\text{ kJ mol}^{-1}$ for $[\text{Mg}(\text{NH}_3)_6](\text{ClO}_4)_2$ [23], $E_a = 4.5\text{ kJ mol}^{-1}$ for $[\text{Co}(\text{NH}_3)_6](\text{ClO}_4)_3$ [24] and $E_a = 2.0\text{ kJ mol}^{-1}$ for $[\text{Cd}(\text{NH}_3)_6](\text{ClO}_4)_2$ [25].

The low value of E_a suggests that the reorientation of the $\text{NH}_3(\text{ND}_3)$ ligands takes effect as a result of a mechanism of the translation–rotation coupling (phonon–reorientation coupling) [26], which makes the real barrier to the rotation of the $\text{NH}_3(\text{ND}_3)$ not constant

but fluctuating. The classic picture of this interaction may be as follows: the interaction of the translational lattice modes (phonons) with the reorientation leads, from time to time, to a situation in which the ammonia ligands will have sufficient space for the nearly random rotation. Thus, the effective value of the energy activation for the reorientation, determined in that case, will be lower than in the case when the phonon–reorientation coupling does not exist.

It can be seen in Fig. 8 that the FWHM values of the both chosen bands exponentially decrease as the temperature is being reduced down to the phase transitions region and then becomes nearly constant. It probably means that at T_{C1} phase transition the stochastic reorientation of ClO_4^- anions is “frozen”, certainly in the time scale of the optic spectroscopy. The parameters fitted to Eq. (1) are listed in Table 3. The mean value of the activation energy for the reorientation of the ClO_4^- anions is $E_a = 6.6\text{ kJ mol}^{-1}$ (1.6 kcal mol^{-1}) in phase I. The obtained value is very close to those for $[\text{Ni}(\text{NH}_3)_6](\text{ClO}_4)_2$ ($E_a = 6\text{ kJ mol}^{-1}$ [6]). For comparison, the insertion in Fig. 8a also presents FWHM vs. temperature for $[\text{Ni}(\text{NH}_3)_6](\text{ClO}_4)_2$ taken from Ref. [17].

4. Conclusions

1. $[\text{Ni}(\text{ND}_3)_6](\text{ClO}_4)_2$ and $[\text{Ni}(\text{NH}_3)_6](\text{ClO}_4)_2$ have three solid phases at 100–300 K. The phase transition temperatures of the deuterated substance obtained on heating: $T_{C1}^h = 164.1\text{ K}$ and $T_{C2}^h = 145.1\text{ K}$ are shifted, as compared to the non-deuterated one, towards the lower temperatures of ca. 8 and 5 K, respectively.

- The ClO_4^- anions perform a fast, picosecond, isotropic reorientation in the high-temperature phase with the activation energy of ca. 6.6 kJ mol^{-1} (6 kJ mol^{-1} for non-deuterated compound). This reorientation abruptly stops at the phase transitions region.
- The ND_3 ligands perform a fast, picosecond reorientation around the Ni–N bonds in all three detected phases with the activation energy of ca. 2.9 kJ mol^{-1} (4 kJ mol^{-1} for non-deuterated compound). This reorientational motion is only slightly distorted at T_{C1} phase transition, probably due to the slow down of the fast reorientations of the ClO_4^- anions at this phase transition.
- The low value of the effective activation energy ($E_a \approx 3\text{--}4 \text{ kJ mol}^{-1}$) suggests that the reorientation of the ND_3 (NH_3) ligands proceeds through the translation–rotation coupling, which makes the barrier to the rotation of the ammonia ligands not constant but fluctuating.
- Both the polymorphism and the reorientational dynamics of molecular groups are very similar in the deuterated and in the non-deuterated compound. However they are not identical.

Acknowledgments

A part of this work comes from a students' scientific project, and thus we thank Ms. A. Jugowiec, M. Koziń and B. Gruszka for their comprehensive cooperation. Our thanks are also due to Dr. M. Rachwalska from our Faculty for $[\text{Ni}(\text{D}_2\text{O})_6](\text{ClO}_4)_2$. We are very grateful to Professor S. Wróbel who let us make DSC measurements. We also thank Dr. hab. E. Ściesińska and J. Ściesiński M.Sc. from H. Niewodniczański Institute of Nuclear Physics in Kraków for FT-FIR spectra and Dr. A. Weselucha-Birczyńska from the Regional Laboratory of Physicochemical Analysis and Structural Research in Kraków for FT-RS spectrum. We are also grateful to Dr. M. Bučko from the University of Mining and Metallurgy at Kraków for doing the X-ray powder diffraction measurement.

References

- J.M. Janik, J.A. Janik, G. Pytasz, J. Sokołowski, J. Raman Spectrosc. 4 (1975) 13.
- M. Rachwalska, J.M. Janik, J.A. Janik, G. Pytasz, T. Waluga, Phys. Stat. Sol. (a) 30 (1975) K81.
- J.A. Janik, J.M. Janik, K. Otnes, K. Rościszewski, Physica B 83 (1976) 259.
- J.A. Janik, J.M. Janik, K. Otnes, Physica B 90 (1977) 275.
- J.M. Janik, J.A. Janik, A. Migdał-Mikuli, E. Mikuli, K. Otnes, Physica B 168 (1991) 45.
- E. Mikuli, Dynamika molekularna związków typu $[\text{Me}(\text{NH}_3)_6]\text{X}_2$ i $[\text{Me}(\text{H}_2\text{O})_6]\text{X}_2$, rozprawa habil. Nr 300, UJ Kraków, 1995.
- J.M. Janik, J.A. Janik, B. Janik, Acta Phys. Polon. A 49 (1976) 377.
- B. Janik, J.M. Janik, J.A. Janik, J. Raman Spectrosc. 7 (1978) 297.
- S. Hodorowicz, M. Ciechanowicz-Rutkowska, J.M. Janik, J.A. Janik, Phys. Stat. Sol. (a) 43 (1977) 53.
- B. Szczaniecki, L. Laryś, U. Gruszczyńska, Acta Phys. Polon. A 46 (1974) 759.
- M. Krupski, J. Stankowski, Acta Phys. Polon. A 50 (1976) 685.
- M. Krupski, J. Stankowski, Acta Phys. Polon. A 55 (1979) 597.
- E. Dynowska, J. Stankowski, Phys. Stat. Sol. (a) 52 (1979) 381.
- M. Godlewska, M. Rachwalska, J. Therm. Anal. 45 (1995) 1073.
- A. Migdał-Mikuli, E. Mikuli, S. Wróbel, Ł. Hetmańczyk, Z. Naturforsch. 54a (1999) 590k.
- R.W.G. Wyckoff, Crystal Structure, (Chapter 10) New York, 1960.
- J.M. Janik (red), Fizyka chemiczna, PWN Warszawa, 1989, p. 458.
- J.M. Terasse, H. Poulet, J.P. Mathieu, Spectrochim. Acta 20 (1964) 305.
- C. Carabatos-Nédelec, P. Becker, J. Raman Spectrosc. 28 (1997) 663.
- P. da, R. Andrade, A.D. Pasad Rao, R.S. Katiyar, S.P.S. Porto, Solid State Commun. 12 (1973) 847.
- P. da, R. Andrade, S.P.S. Porto, Solid State Commun. 13 (1973) 1249.
- G. Bator, R. Jakubas, J. Baran, Vib. Spectrosc. 25 (2001) 101.
- J.A. Janik, J.M. Janik, A. Migdał-Mikuli, E. Mikuli, K. Otnes, I. Svare, Physica B 97 (1979) 47.
- E. Mikuli, A. Migdał-Mikuli, N. Górka, J. Ściesiński, E. Ściesińska, S. Wróbel, J. Mol. Struct. 651–653C (2003) 519.
- J. Czaplicki, N. Weiden, A. Weiss, Phys. Stat. Sol. (a) 117 (1990) 555.
- K.H. Michel, J. Naudts, J. Chem. Phys. 67 (1977) 547.